# SUPPORTING MATERIALS

# Impaired Transcriptional Response of the Murine Heart To Cigarette Smoke in the Setting of High Fat Diet and Obesity.

Susan Tilton, Norman J. Karin, Bobbie-Jo M. Webb-Robertson, Katrina M. Waters, Vladimir Mikheev K. Monica Lee , Richard A. Corley, Joel G. Pounds, and Diana J. Bigelow

Pacific Northwest National Laboratory & Battelle Toxicology Northwest,
Richland, WA 99352

**Table S1: Body Weights and Blood Carboxyhemoglobin (COHb) Levels in Mice**

| | | RW | | | DIO | | |
|---|---|---|---|---|---|---|---|
| | Study Day[a] | SC | MS | SS | SC | MS | SS |
| Body Weight[b] (g) | 1 | 28.9±1.2 | 29.1±1.6 | 28.9±1.8 | 35.5±2.4 | 34.8±2.8 | 35.2±2.9 |
| | 11 | 27.0±1.2 | 26.8±1.6 | 26.1±1.9 | 31.8±2.1 | 32.5±2.9 | 32.1±2.6 |
| Blood COHb[b] (%) | 10 | 1.5±0.1 | 29.0±1.4[c] | 29.6±1.0[c] | 1.5±0.1 | 26.4±1.5[c,d] | 29.8±1.0[c,d] |

Abbreviations: RW, regular weight; DIO, diet-induced obese; SC, sham control; MS, mainstream cigarette smoke; SS, sidestream cigarette smoke; CO-Hb, carboxyhemoglobin.

[a]Study Day 1 indicates the first day of smoke or filtered air exposure; CO-Hb was taken immediately after the last exposure (Day 10); and terminal body weights were measured on the next day following the last exposure (Day 11).

[b]Values represent means ±SD; n=8 for each group

[c]$p<0.05$ relative to the corresponding SC group.

[d]$p<0.05$ vs. corresponding RW group.

**Table S2: Chamber Exposure Conditions**[a]

| Property | MS | SS |
|---|---|---|
| WTPM (μg/L) | 254.9 ± 10.6 | 82.0 ± 6.7 |
| CO (ppm) | 251.2 ± 6.6 | 276.1 ± 8.8 |
| MMAD (μm) | 0.59 | 0.22 |
| GSD (μm) | 1.30 | 1.58 |

[a]Abbreviations: MS, mainstream cigarette smoke; SS, sidestream cigarette smoke; WTPM, wet weight total particulate matter; CO, carbon monoxide; MMAD, mass median aerodynamic diameter of smoke particles; GSD, geometric standard deviation of MMAD. Values represent means ± SD, where applicable.

***Animal Exposures.*** Mice were acclimated to the AALAS-accredited animal facility as well as to the nose-only inhalation exposure restraint tubes for one week prior to the initiation of smoke exposures. Animal rooms maintained a temperature of 22 ± 2 °C and relative humidities of 35 to 70%; a 12-hour light cycle began with lights starting at 0600 hr. Feed and water were provided *ad libitum*. Health screens were performed on sentinel mice; terminal health monitoring of all mice included serological testing for antibodies to common rodent pathogens.

***Inhalation chambers and exposure monitoring***. Mice were exposed to either MS or SS smoke or filtered air using a Jaeger-Baumgartner 2070i cigarette-smoking machine (JB2070 CSM; CH Technologies, Westwood, NJ) modified to provide simultaneous generation of MS and SS smoke from 3R4F reference cigarettes (Univ. of Kentucky, Lexington). Each nose-only exposure chamber port received an average of at least 450 ml/min of exposure atmosphere for a total chamber flow rate of ~40 L/min. Each chamber was housed in vented enclosures to contain the exposures. Cigarette smoke concentrations (μg WTPM/L) were determined gravimetrically from duplicate filter samples collected during the 1$^{st}$, 3$^{rd}$, and 5$^{th}$ hour of each total 5-hr exposure period. Smoke samples were collected on Cambridge-style 47-mm glass fiber filters at sampling rates slightly less (~10%) than the maximum flow rate through the individual nose ports for approximately one hr for each sample. Continuous monitoring of particulates was performed using a real-time aerosol monitor (RAM, Microdust Pro, Casella Cel Ltd., Bedford, UK). CO levels, controlled by adjusting chamber dilution air, were analyzed with an on-line CO analyzer (California Analytic Instruments, Orange, CA). Chamber temperature and relative humidity were determined at a representative nose port using a solid-state integrated humidity and temperature transmitter (HUMITTER, Vaisala Inc., Woburn, MA). MS particle size distribution was measured using a Mercer-style cascade impactor (InTox Products, Moriarty, NM) with the cut-off range of ~0.4 – 2.5 μm. Particle diameters and their geometric standard deviations were determined by probit analysis. The SS particle concentration and size distribution was monitored using the scanning mobility particle sizer (model 3936L76, TSI, St. Paul, MN).

**Figure S1: Bronchoaveolar Lavage Fluid Cytology from Mice.** Normal weight (RW) and diet-induced obese (DIO) mice exposed to MS or SS smoke, or to HEPA filtered air, i.e., sham controls (SC) exhibited inflammatory and immune cell counts (per 100 μL cell suspension). Cells, visualized and counted under the microscope as described in Experimental Methods, included pulmonary alveolar macrophages (light gray bars) and neutrophils (dark gray bars). Bar heights and error bars represent the means and SEM of each value; asterisks indicate statistical significant differences relative to the appropriate sham control.

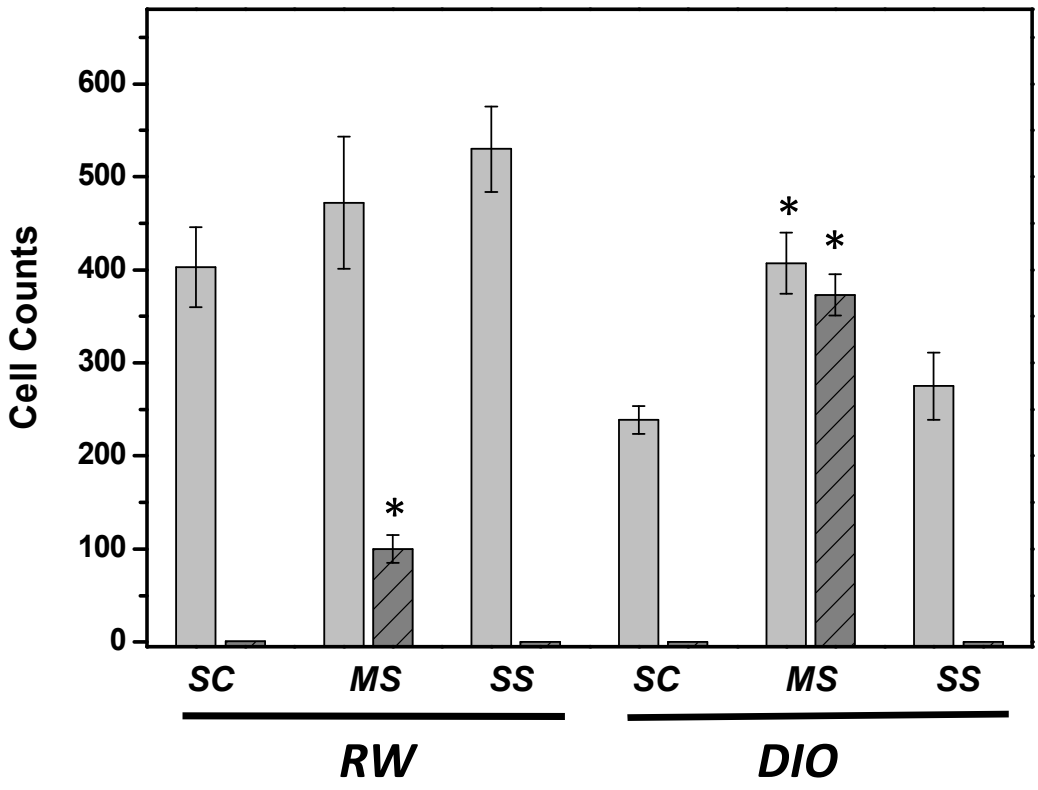


**Figure S1**

**Figure S2: Comparisons and Hierarchical Clustering of Cardiac and Pulmonary Genes Regulated By Diet or Smoke Exposure**. As illustrated by the Venn diagram (Panel A), 3012 genes in the lung and 3,252 genes in the heart were significantly regulated ($p<0.01$, 5% FDR) across the study in RW or DIO mice exposed to MS or SS cigarette smoke or filtered air (SC). All gene expression comparisons were to RW-SC. Lung and heart shared 580 common gene changes based on statistical filter ($p<0.01$). These 580 common genes in heart and lung tissues underwent bidirectional hierarchical clustering (Panel B), shown in the form of a heatmap, the values are log2 fold change for all treatments; red, green, and black represent up-regulated, down-regulated and unchanged genes, respectively. Complete sets of cardiac and pulmonary regulated genes are tabulated in Supplementary Table 1. Unsupervised bidirectional hierarchical clustering of microarray data was performed using Euclidean distance metric and centroid-linkage clustering to group treatments and gene expression patterns by similarity. The clustering algorithms, heat map visualizations and centroid calculations were performed with Multi-Experiment Viewer software based on log2 expression ratio values.

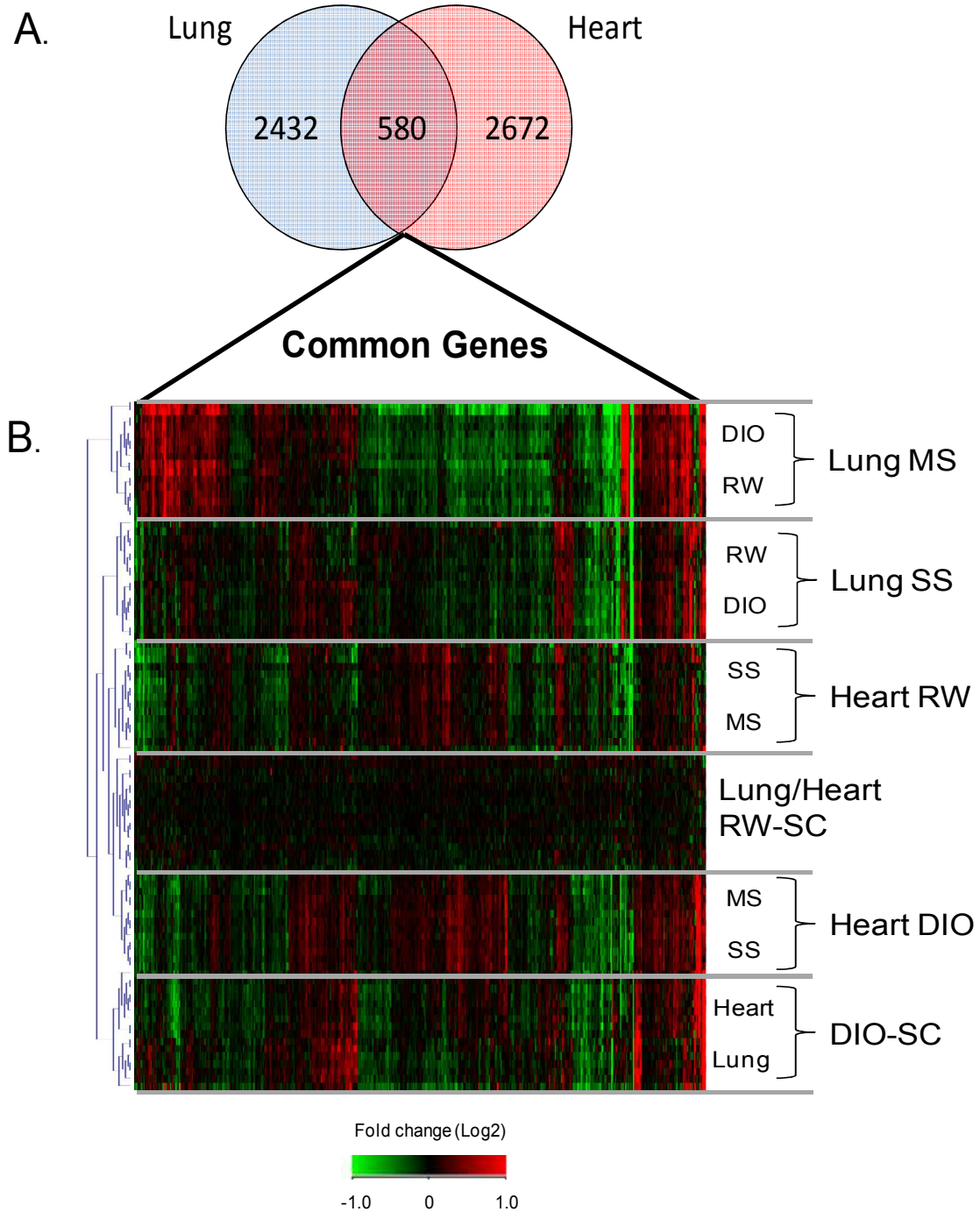
A.
Lung
Heart
2432
580
2672
Common Genes
B.
DIO
RW
Lung MS
RW
DIO
Lung SS
SS
MS
Heart RW
Lung/Heart
RW-SC
MS
SS
Heart DIO
Heart
Lung
DIO-SC
Fold change (Log2)
-1.0
0
1.0

**Figure S2**

**Figure S3:** Comparison of Smoke and Diet Induced-Obesity Related Cardiac Gene Processes in Mice. Functional enrichment of gene processes by high fat diet-induced obesity (DIO-SC), or MS- or SS-smoke exposure in the hearts of RW (RW-MS, RW-SS) and DIO (DIO-MS, DIO-SS) mice using the DAVID functional annotation tool to measure gene enrichment in biological process Gene Ontology (GO) category terms for significant genes compared with background, in this case, RW mice exposed to filtered air, i.e., sham controls. GO category terms are listed with enrichment functions based on p-values according to the black body scale for the p-value (as indicated by the bar below), where black is lowest and white is highest p-value. A complete list of genes within each process is available in Support Table S3.

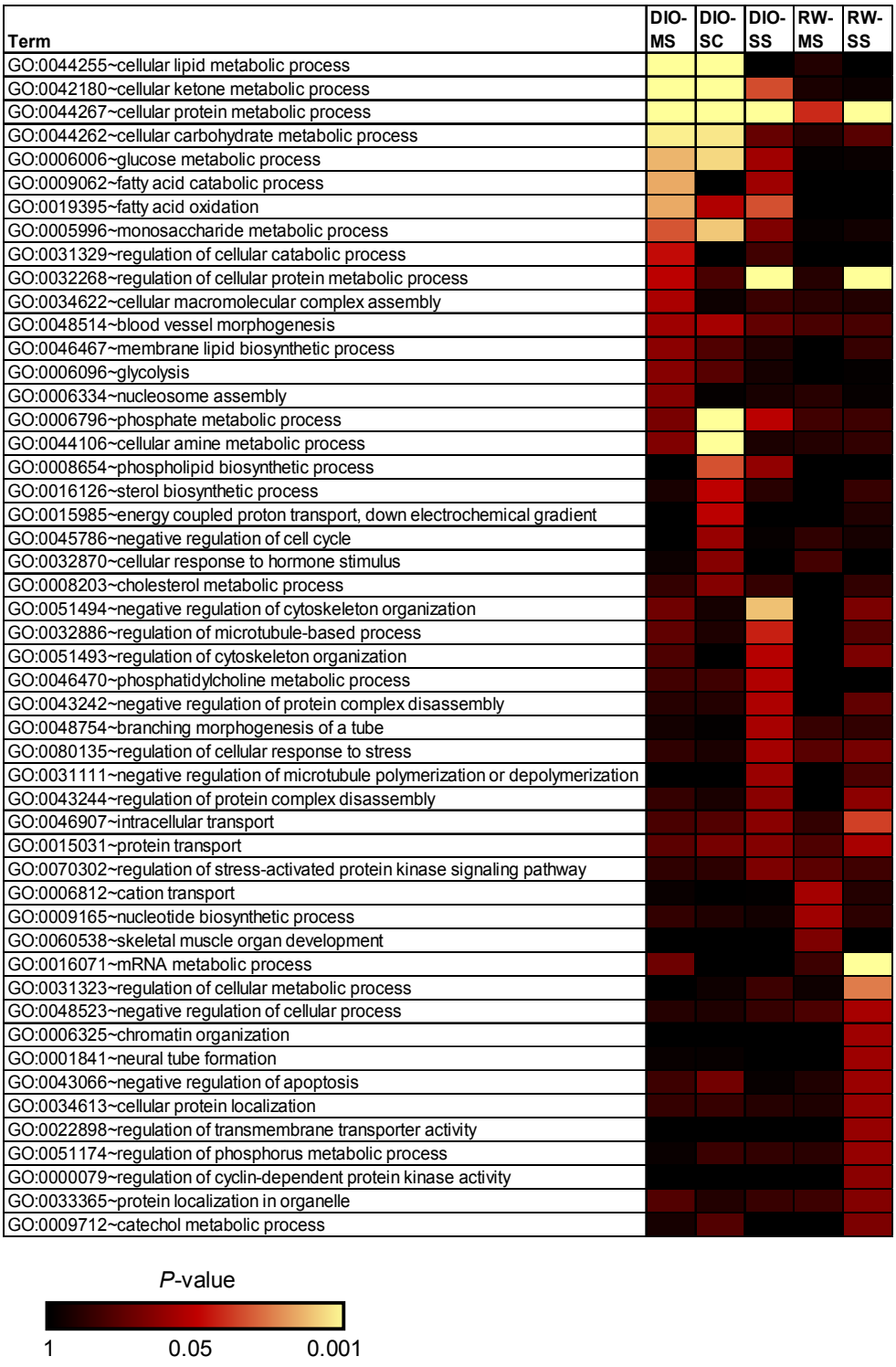
Term
DIO-MS
DIO-SC
DIO-SS
RW-MS
RW-SS
GO:0044255~cellular lipid metabolic process
GO:0042180~cellular ketone metabolic process
GO:0044267~cellular protein metabolic process
GO:0044262~cellular carbohydrate metabolic process
GO:0006006~glucose metabolic process
GO:0009062~fatty acid catabolic process
GO:0019395~fatty acid oxidation
GO:0005996~monosaccharide metabolic process
GO:0031329~regulation of cellular catabolic process
GO:0032268~regulation of cellular protein metabolic process
GO:0034622~cellular macromolecular complex assembly
GO:0048514~blood vessel morphogenesis
GO:0046467~membrane lipid biosynthetic process
GO:0006096~glycolysis
GO:0006334~nucleosome assembly
GO:0006796~phosphate metabolic process
GO:0044106~cellular amine metabolic process
GO:0008654~phospholipid biosynthetic process
GO:0016126~sterol biosynthetic process
GO:0015985~energy coupled proton transport, down electrochemical gradient
GO:0045786~negative regulation of cell cycle
GO:0032870~cellular response to hormone stimulus
GO:0008203~cholesterol metabolic process
GO:0051494~negative regulation of cytoskeleton organization
GO:0032886~regulation of microtubule-based process
GO:0051493~regulation of cytoskeleton organization
GO:0046470~phosphatidylcholine metabolic process
GO:0043242~negative regulation of protein complex disassembly
GO:0048754~branching morphogenesis of a tube
GO:0080135~regulation of cellular response to stress
GO:0031111~negative regulation of microtubule polymerization or depolymerization
GO:0043244~regulation of protein complex disassembly
GO:0046907~intracellular transport
GO:0015031~protein transport
GO:0070302~regulation of stress-activated protein kinase signaling pathway
GO:0006812~cation transport
GO:0009165~nucleotide biosynthetic process
GO:0060538~skeletal muscle organ development
GO:0016071~mRNA metabolic process
GO:0031323~regulation of cellular metabolic process
GO:0048523~negative regulation of cellular process
GO:0006325~chromatin organization
GO:0001841~neural tube formation
GO:0043066~negative regulation of apoptosis
GO:0034613~cellular protein localization
GO:0022898~regulation of transmembrane transporter activity
GO:0051174~regulation of phosphorus metabolic process
GO:0000079~regulation of cyclin-dependent protein kinase activity
GO:0033365~protein localization in organelle
GO:0009712~catechol metabolic process
P-value
1
0.05
0.001

**Figure S3**